Electronic Supplementary Material (ESI) for ChemComm.

Free-standing Pt-Ni nanowires catalyst for H_2 generation from hydrous hydrazine

Yu-Ping Qiu,† Liang-Liang Zhou,† Qing Shi and Ping Wang*

School of Materials Science and Engineering, South China University of Technology, Guangzhou 510641, P.R. China

*Corresponding author. E-mail: mspwang@scut.edu.cn

† These authors contributed equally to this work.

Experimental section

Catalyst preparation

Pt-Ni nanowire samples with tunable compositions were synthesized using a solvothermal method. In a typical procedure, the mixture of chloroplatinic acid ($H_2PtCl_6 \cdot H_2O$, Pt content ≥37.5%) and nickel acetylacetonate ($Ni(acac)_2$, 95%) with varied molar ratios together with 20 mmol of potassium hydroxide (KOH, 97%) were dissolved in 30 mL of 1:1 (v/v) mixture of N,N-dimethylmethanamide (DMF, 99.8%) and ethylene glycol (EG, 98%) under magnetic stirring and sonication at room temperature for 4 h. The yielded transparent solution was then transferred into a 50 ml Teflon-lined autoclave and heated at 170 °C for 4 h with no intentional control of ramping or cooling rate. The collected product by centrifugation at 6000 rpm was thoroughly washed with deionized (DI) water (with a resistivity of 18 MΩ at 25 °C) and ethanol and finally dried at 60 °C under dynamic vacuum for 6 h. For comparison, pure Ni catalyst was fabricated by reduction of NiO at 300 °C under H_2 atmosphere for 1 h, and a physical mixture sample was also fabricated by grinding the powder mixture of pure Pt and Ni with a molar ratio of 3:2.

Catalyst characterization

The phase structure of the catalyst samples was analyzed by X-ray diffraction (XRD) on a Rigaku RINT 2000 instrument. The morphology and microstructure of the samples were characterized by transmission electron microscopy (TEM, JEOL-2100F) equipped with an energy dispersive X-ray spectroscopy (EDS) unit. The surface composition and chemical states of the constituent elements of the catalysts were analyzed using X-ray photoelectron spectroscopy (XPS, Thermo Scientific K-ALPHA$^+$). In the XPS analyses, the binding energies (BEs) were calibrated against the C 1s line at 284.8 eV of the adventitious carbon. A quantitative elemental analysis was conducted by inductively coupled plasma-atomic emission spectrometry (ICP-AES) on an Iris Intrepid instrument. The on-line thermogravimetric-mass spectrometry (TG-MS) analyses of the gases evolved from the sample were conducted using a Netzsch STA449F3-QMS403 thermal analyses system.

Catalytic performance testing

The catalytic properties of the catalysts towards $N_2H_4 \cdot H_2O$ decomposition were measured in a two-necked round-bottomed flask. In a typical run, the flask containing

the catalyst and an alkaline aqueous solution was preheated and hold at the designated temperature under magnetic stirring. After injection of $N_2H_4 \cdot H_2O$ into the flask, the decomposition reaction was immediately initiated. The generated gaseous products were allowed to pass through a 1.0 M hydrochloric acid (HCl) solution to absorb ammonia, if any, and were then measured by the water-displacement method using an electronic balance with a precision of ±0.01 g. All the measurements were carried out in a solution of 0.50 M $N_2H_4 \cdot H_2O$ and 2.0 M NaOH and the molar ratio of $N_2H_4 \cdot H_2O$ to catalyst was fixed at 13:1. The H_2 selectivity (X) was calculated following Eq 1, which was derived from the equations describing the decomposition reactions of $N_2H_4 \cdot H_2O$. The reaction rate at a conversion level of 50% was determined, assuming that all the Ni atoms take part in the catalytic reaction.

$$X = \frac{3Y - 1}{8}\left[Y = \frac{n(N_2 + H_2)}{n(N_2H_4)}\right] \qquad (1)$$

The turnover frequency (TOF) was calculated from Eq. 2,

$$TOF = \frac{n_{N_2H_4}}{n_{metal} \times t} \qquad (2)$$

where $n(N_2H_4)$ is the consumed quantity of N_2H_4 when the conversion reaches 50%, n(metal) is the quantity of active metal atoms in the catalyst, and t is the reaction time at a conversion of 50%. In the present study, the TOF values were calculated based on Ni, Pt and Ni+Pt atoms, respectively.

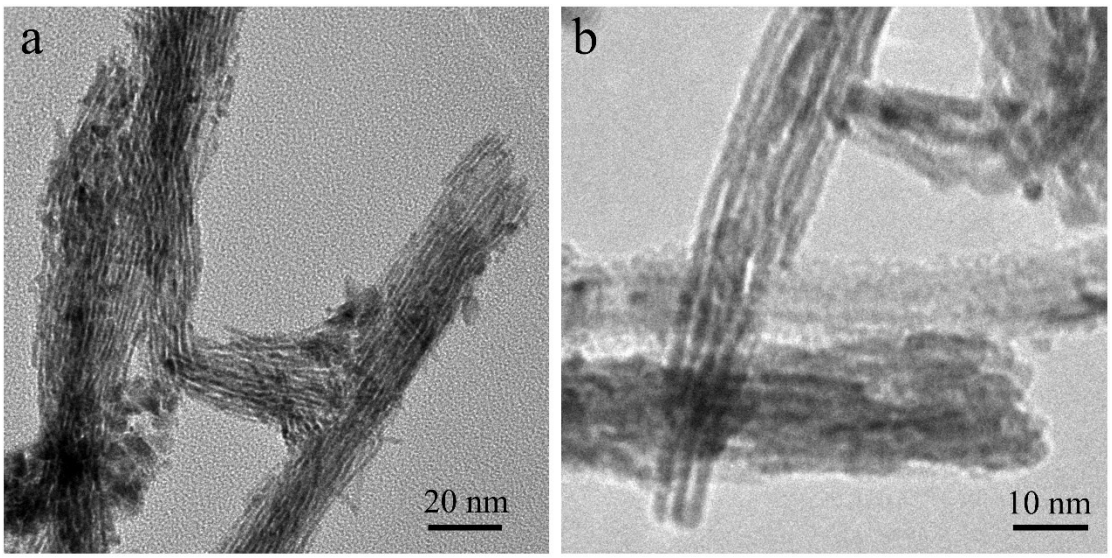

Fig. S1 Representative TEM images of Pt_3Ni_2 nanowires sample.

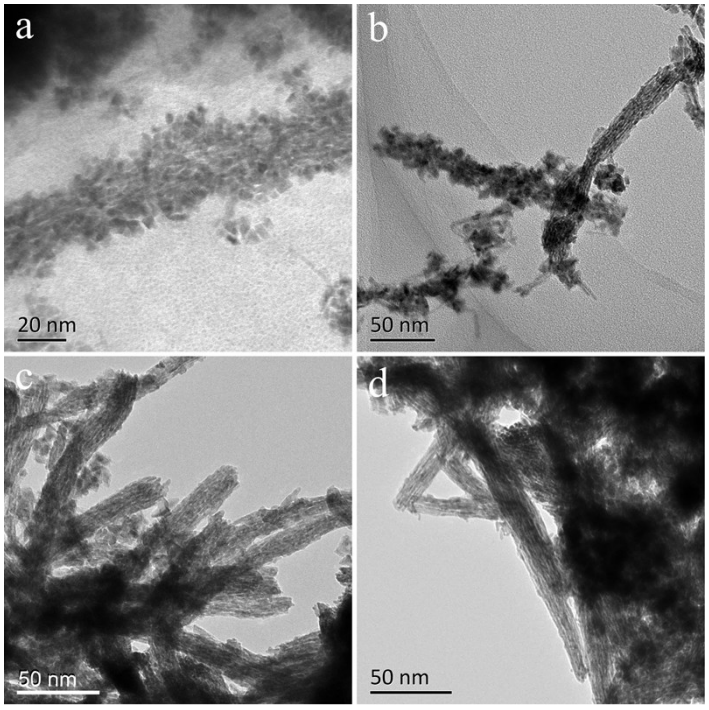

Fig. S2 TEM images of the Pt_3Ni_2 samples collected at different reaction durations. (a) 10 min; (b) 1 h; (c) 4 h; (d) 8 h.

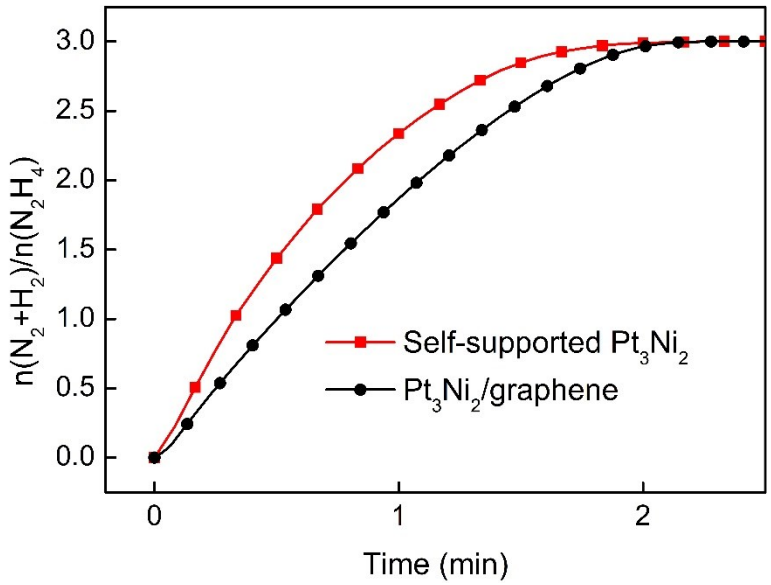

Fig. S3 Kinetic curves of $N_2H_4 \cdot H_2O$ decomposition over self-supported Pt_3Ni_2 and Pt_3Ni_2/graphene catalysts at 50 °C. The measurements were conducted in 1 mL of aqueous solution containing 0.50 M $N_2H_4 \cdot H_2O$ and 2.0 M NaOH. The catalyst/$N_2H_4 \cdot H_2O$ molar ratio was fixed at 1:13. It was observed that the two catalysts showed similar catalytic performance towards $N_2H_4 \cdot H_2O$ decomposition.

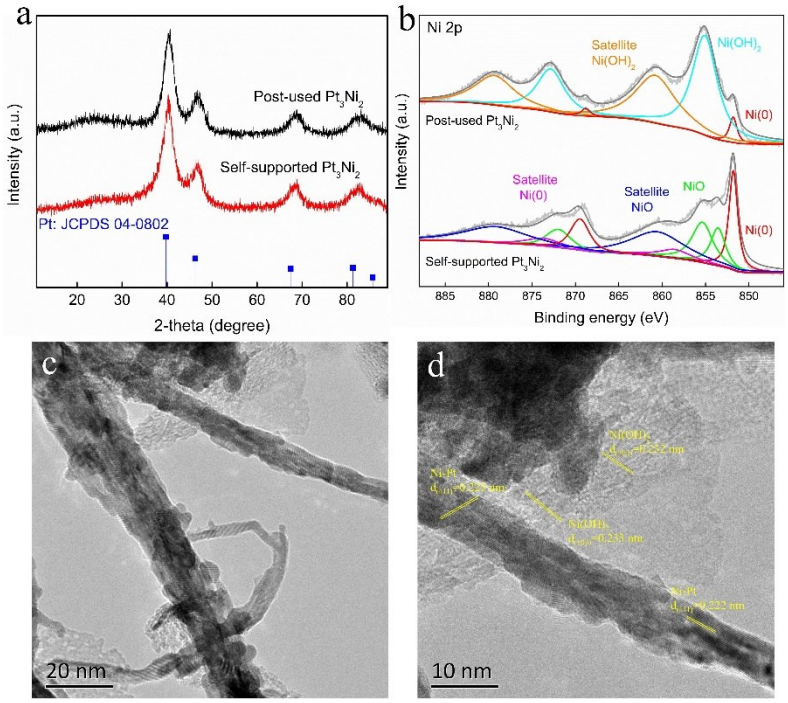

Fig. S4 (a) XRD patterns and (b) XPS spectra of the as-prepared and post-used Pt_3Ni_2 nanowires catalyst; (c, d) TEM images at different magnifications of the post-used Pt_3Ni_2 nanowires catalyst.

Table S1. Chemical composition of the catalysts.

Catalyst	Pt/Ni atomic ratio
PtNi nanowires[a]	1.19
Pt_3Ni_2 nanowires (as-prepared)[a]	1.86
Pt_3Ni_2 nanowires (as-prepared)[b]	1.68
Pt_3Ni_2 nanowires (post-used)[b]	1.73
Pt_3Ni nanowires[a]	4.35

[a] Determined by ICP-AES.
[b] Determined by XPS.

Table S2. A comparison of catalytic performance of self-supported Pt_3Ni_2 nanowires and relevant catalysts reported in literatures for $N_2H_4 \cdot H_2O$ decomposition.

Catalyst	Temperature (°C)	TOF (h^{-1})[a]	TOF (h^{-1})[b]	TOF (h^{-1})[c]	Ref.
$Rh_{0.8}Ni_{0.2}$/MIL-101	50	/	/	428.6	1
$Ni_{60}Pt_{40}$/NC	50	1602	/	/	2
$NiPt_{0.057}/Al_2O_3$	30	16.5	/	/	3
$Rh_{47}Ni_{18}P_{35}$@MOF-74	50	/	/	715.4	4
$Rh_{58}Ni_{42}$@MIL-101	50	/	/	344	5
$Pt_{0.5}Ni_{0.5}$/NGNs-850	50	/	/	943	6
$(Ni_3Pt_7)_{0.5}$-$(MnO_x)_{0.5}$/NPC	50	/	/	706	7
$Ni_{0.6}Pt_{0.4}$–MoO_x	50	/	/	822	8
Pt_3Ni_2 nanowires	50	726	484	290	This work

[a] Calculated based on Ni atoms.
[b] Calculated based on noble metal atoms.
[c] Calculated based on Ni and noble metal atoms.

References

1. Z. Zhang, S. Zhang, Q. Yao, G. Feng, M. Zhu and Z. H. Lu, *Inorg. Chem. Front.*, 2018, **5**, 370.
2. Y. P. Qiu, Q. Shi, L. L. Zhou, M. H. Chen, C. Chen, P. P. Tang, G. S. Walker and P. Wang, *ACS Appl. Mater. Interfaces*, 2020, **12**, 18617.
3. L. He, Y. Huang, A. Wang, Y. Liu, X. Liu, X. Chen, J. J. Delgado, X. Wang and T. Zhang, *J. Catal.*, 2013, **298**, 1.
4. R. Jiang, X. Qu, F. Zeng, Q. Li, X. Zheng, Z. Xu and J. Peng, *Int. J. Hydrogen Energy*, 2019, **44**, 6383.

5. P. Zhao, N. Cao, W. Luo and G. Cheng, *J. Mater. Chem. A*, 2015, **3**, 12468.
6. A. Kumar, X. Yang and Q. Xu, *J. Mater. Chem. A*, 2019, **7**, 112.
7. B. Xia, T. Liu, W. Luo and G. Cheng, *J. Mater. Chem. A*, 2016, **4**, 5616.
8. Q. Yao, M. He, X. Hong, X. Zhang and Z. H. Lu, *Inorg. Chem. Front.*, 2019, **6**, 1546.